

EQUILIBRIUM TRANSPORT OF SHEET ELECTRON BEAMS IN SOLENOIDAL FOCUSING FIELDS*

R. Pakter[#]

Instituto de Física, Universidade Federal do Rio Grande do Sul, Brazil

Abstract

The transport of sheet electron beams is an important issue in the development of high-power RF generators because large amounts of current can be achieved at reduced space-charge density. In this paper we analyze equilibrium configurations for the transport of sheet electron beams in tapered solenoidal focusing fields. In particular, we use the generalized envelope equations obtained for the evolution of space-charge-dominated beams propagating through a general linear focusing channel [R. Pakter and C. Chen, Phys. Rev. E, 62, 2789 (2000)] to derive an optimal focusing field profile for sheet beam transport. Analytic solutions based on multi-time scale perturbation theory are found and compared to numerical simulations.

INTRODUCTION

The improvement of high-power vacuum microwave sources plays a crucial role in the development of the new generation of high-gradient, high-frequency particle accelerators [1]. As scaling up the microwave sources to higher frequencies, a significant difficulty is the need to transport intense beams through decreasing aperture sizes, because the RF circuit dimensions decrease with the wavelength. In this regard, the use of sheet electron beams seems a promising concept, since larger amounts of current can be transported at lower current densities by increasing the width of the beam, while keeping its height of the order the RF wavelength [2-4]. The main drawback on the use of sheet beams in comparison to the usual round beam is that the sheet beam may be more vulnerable to some instabilities in ordinary solenoidal focusing channels [5].

In this paper, we analyze the transport of sheet electron beams in solenoidal focusing systems. In particular, we consider the case of tapered focusing fields, and search for field profiles leading to equilibrium solutions for the transport. Use is made of the generalized envelope equations obtained for the evolution of intense beams in general linear focusing systems [6] to derive an equation for the magnetic field profile as a function propagation distance.

MODEL AND THE GENERALIZED ENVELOPE EQUATIONS

In this section we review the generalized envelope

equations [6], specializing to the transport in solenoidal focusing fields. Let us consider a thin, continuous, space-charge-dominated beam propagating with constant axial velocity $\beta_b c \hat{e}_z$ through a solenoidal focusing field. Here, c is the speed of light in vacuum. The focusing magnetic field is approximated by

$$\mathbf{B}_0(\mathbf{x}) = B_z(s) \hat{e}_z - \frac{1}{2} B'_z(s) (x \hat{e}_x + y \hat{e}_y) \quad (1)$$

where $s = z = \beta_b ct$ is the axial coordinate, and the prime denotes derivative with respect to s .

It has been shown in the paraxial approximation that there exists a class of solutions to steady-state cold-fluid equations [6], which, in general, describes corkscrewing elliptic beam equilibria for, space-charge-dominated beam propagating through the applied focusing magnetic field defined in Eq. (1). The generalized beam envelope equations are [6]

$$a'' + \left(\frac{b^2(\alpha_x^2 - 2\alpha_x\alpha_y) + a^2\alpha_y^2}{a^2 - b^2} - 2\alpha_y\sqrt{\kappa_z(s)} \right) a - \frac{2K}{a+b} = 0 \quad (2)$$

$$b'' - \left(\frac{a^2(\alpha_y^2 - 2\alpha_x\alpha_y) + b^2\alpha_x^2}{a^2 - b^2} + 2\alpha_x\sqrt{\kappa_z(s)} \right) b - \frac{2K}{a+b} = 0, \quad (3)$$

$$\frac{1}{b} \frac{d}{ds} \left\{ b^2 [\alpha_x + \sqrt{\kappa_z(s)}] \right\} - \frac{a^3(\alpha_x - \alpha_y)}{a^2 - b^2} \frac{d}{ds} \left(\frac{b}{a} \right) = 0, \quad (4)$$

$$\frac{1}{a} \frac{d}{ds} \left\{ a^2 [\alpha_y + \sqrt{\kappa_z(s)}] \right\} - \frac{b^3(\alpha_x - \alpha_y)}{a^2 - b^2} \frac{d}{ds} \left(\frac{a}{b} \right) = 0, \quad (5)$$

$$\frac{d\theta}{ds} - \frac{a^2\alpha_y - b^2\alpha_x}{a^2 - b^2} = 0. \quad (6)$$

where $\sqrt{\kappa_z(s)} = qB_z(s)/2\gamma_b\beta_b mc^2$ is the focusing parameters for the solenoidal and quadrupole-focusing magnetic fields, $K = 2q^2 N_b / \gamma_b^3 \beta_b^2 mc^2$ is the normalized self-field perveance, $a(s)$, $b(s)$, and $\theta(s)$ are the major radius, the minor radius, and the angle of rotation with respect to the laboratory frame of the ellipse that describes the cold-fluid corkscrewing elliptic beam equilibrium density illustrated in Fig. 1, and the variables $\alpha_x(s)$ and $\alpha_y(s)$ specify the corresponding equilibrium flow velocity as defined in Refs. 6. Here, m and q are the rest mass and charge of the particle, N_b is the number of particles per unit axial length, and $\gamma_b = (1 - \beta_b^2)^{-1/2}$ is the relativistic mass factor.

* Work supported by CNPq and CAPES, Brazil.

[#] pakter@if.ufrgs.br. The author would like to thank the partial support from the PAC03 Organizing comity.

In general, the envelope equations (2)-(6) are used to determine beam evolution for a given external focusing field. In the case of sheet electron beams in solenoidal focusing field to be discussed in the next section, we apply the generalized envelope equations to determine field profiles that lead to equilibrium beam transport, given the required constrains on the beam evolution.

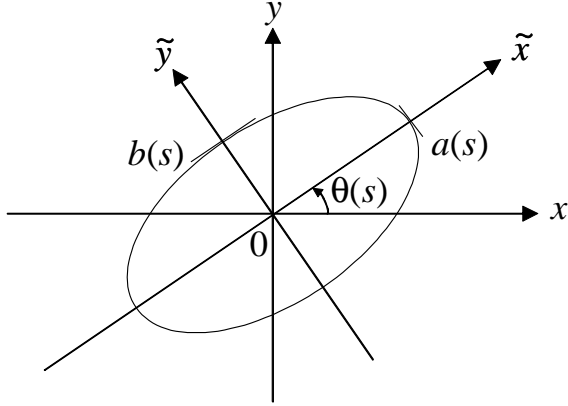


Figure 1: equilibrium density profile in the laboratory and rotating coordinate systems.

SHEET BEAM TRANSPORT IN SOLENOIDAL FIELD

In the case of sheet electron beams, the ellipsis that describes the equilibrium beam density has one of the axis much greater than the other, i.e. $a \gg b$, and its is required that the beam does not rotate, such that the conditions $\theta(s) = 0$, $d\theta(s)/ds = 0$ must be satisfied throughout the focusing channel. From Eq. (6) it is seen that this condition implies that $a(s)$, $b(s)$, $\alpha_x(s)$ and $\alpha_y(s)$ are not independent anymore, but must satisfy

$$a^2 \alpha_y^2 = b^2 \alpha_x^2 \quad (7)$$

for all s . Therefore, the task that we propose here is to determine a solenoidal focusing field profile that guarantees the condition imposed by Eq. (7).

Using Eq. (7), and keeping only the leading order terms of a/b , the generalized envelope equations can be written as

$$\frac{d^2 a}{ds^2} - \frac{(\alpha_x + \Omega_L) b^2 \alpha_x + 2K}{a} = 0, \quad (8)$$

$$\frac{d^2 b}{ds^2} - \Omega_L \alpha_x b = \frac{2K}{a}, \quad (9)$$

$$\frac{d}{ds} [b^2 (2\alpha_x + \Omega_L)] = 2\alpha_x b \frac{db}{ds}, \quad (10)$$

$$\frac{d}{ds} (a^2 \Omega_L) + 4\alpha_x b \frac{db}{ds} = 0 \quad (11)$$

where $\Omega_L(s) = 2\sqrt{\kappa_z(s)}$ is the Larmor frequency, which is proportional to the focusing field strength. The set of equations (8)-(11) describe the evolution of a nonrotating

sheet beam, where, specifically, the field profile $\Omega_L(s)$ is determined by Eq. (11).

Examining Eqs. (8)-(11) one notices that the large disparity in the transverse beam length scales along the major and minor axis, $a \gg b$, also leads to a large disparity in the longitudinal length scales involved in the evolution of the envelope variables. In particular, equations (9) and (10) describe *fast* variations for $b(s)$ and $\alpha_x(s)$, whereas, equations (8) and (11) describe *slow* variations for $a(s)$ and $\Omega_L(s)$ [7]. Therefore, we can obtain approximate solutions to the envelope equations by first integrating the fast equations in time scales where the variations of the slow variables are negligible, and then solving the slow equations by averaging over the fast time scales.

Assuming Ω_L constant, we directly integrate Eq. (10) to obtain

$$b(\alpha_x + \Omega_L) = \text{const.} \quad (12)$$

In principle, the above constant could vary on the slow-time scale, however more detailed calculations show that it is a real constant. Physically, this constant is related to the differential rotation between the internal beam particle flow given by α_x (see Ref. 6) and the Larmor frequency. Here, we are interested in typical cases where the particles move with the Larmor frequency, such that the constant in Eq. (12) is equal to 0.

Using Eq. (12) and assuming a and Ω_L constants, we can solve Eq. (9) to find

$$b(s) = A \cos(\Omega_L s + \phi) + \frac{2K}{\Omega_L^2 a} \quad (13)$$

which gives the evolution for the ellipsis minor radius. From Eq. (13) we notice that the fast-time scale is governed by the local Larmor frequency Ω_L .

Using Eqs. (12) and (13) in Eqs. (8) and (11), and averaging over the fast time scales, we obtain

$$\frac{d^2 a}{ds^2} - \frac{2K}{a} = 0, \quad (14)$$

$$\frac{d}{ds} (a^2 \Omega_L) = 0. \quad (15)$$

Many aspects of sheet beam evolution in solenoidal focusing can be understood from Eqs. (14) and (15). First, the evolution of the slow variables is completely independent of fast variables, such that, as long as the two-time-scale analysis is valid, the field profile and the major ellipsis radius will be the same irrespective to the minor radius and internal beam flow detailed characteristics. Second, the focusing field strength must be proportional to the inverse of the square of the major radius in order to preserve the sheet beam from rotating. In fact, from Eq. (15) we obtain

$$\Omega_L(s) = \frac{a_o^2 \Omega_{Lo}}{a^2(s)}, \quad (16)$$

where $a_o = a(0)$ and $\Omega_{Lo} = \Omega_L(0)$ are the initial conditions at the entrance of the focusing channel. Third,

the major radius evolution is governed exclusively by space-charge forces which are always defocusing. Hence, to increase the interaction region it is convenient to inject a converging beam with $a'_o \equiv da/ds|_{s=0} < 0$. The particular value of a'_o for a specific arrangement can be calculated with the aid of Eq. (14). Multiplying Eq. (14) by da/ds and integrating leads to

$$\frac{1}{2} \left(\frac{da}{ds} \right)^2 - 2K \ln a = \text{const.} \quad (17)$$

Let us consider a case where we inject in the focusing channel a beam with major radius a_o , let the beam converge to a minimum major radius a_{\min} , and extract the beam when its major radius returns to its initial value; i.e., $a(S) = a_o$, where S is the length of the focusing channel. In this situation, the required initial beam convergence is given by Eq. (17) as

$$a'_o = -2 \left(K \ln \frac{a_o}{a_{\min}} \right)^{1/2}. \quad (18)$$

Fourth, the focusing channel length S can also be estimated from Eq. (14) as

$$S \approx \left(\frac{a_o^2 - a_{\min}^2}{K} \right)^{1/2}. \quad (19)$$

In reality, S is a measure of the slow time scale associated with the dynamics of $a(s)$ and $\Omega_L(s)$. Recalling that the fast time scale is governed by the Larmor frequency, the condition of validity for the multiple time-scales analysis applied here is $\overline{\Omega}_L S \gg 1$, with the bar indicating average values. Using Eq. (19) the condition roughly leads to

$$K \ll \overline{\Omega}_L^2 \bar{a}^2, \quad (20)$$

which informs that for a given focusing field and beam size, there is a limit in the total beam intensity. In practice this is not a strong constrain because the whole purpose of using sheet beams is being able to reduce beam intensity by spreading it over larger sizes by increasing the ellipsis major radius. Finally, using Eqs. (14) and (16) we can write down

$$\frac{d^2 \Omega_L}{ds^2} - \frac{3}{2 \Omega_L} \left(\frac{d \Omega_L}{ds} \right)^2 + \frac{4 K \Omega_L^2}{a_o^2 \Omega_{Lo}} = 0 \quad (21)$$

which gives the optimal solenoidal focusing field profile $\Omega_L(s)$ that leads to an equilibrium nonrotating sheet beam propagation.

The above results were tested against solutions obtained by numerically integrating the generalized envelope equations using the focusing field profile prescribed by Eq. (21). A good agreement was found between the numerical solutions and the estimates from the multiple-time-scale analysis. In particular, considering moderately intense sheet electron beams with $K \sim 10^{-2}$ and major radius of a few centimeters, transported along the typical longitudinal length scales of high-power vacuum microwave sources (on the order of 30 cm), presented very small rotation angles on the order of 10^{-4} rad.

CONCLUSIONS

We have analyzed equilibrium configurations for the transport of sheet electron beams in tapered solenoidal focusing fields. In particular, using the generalized envelope equations obtained for the evolution of space-charge-dominated beams propagating through a general linear focusing channel, we derived an equation that provides an optimal focusing field profile for nonrotating sheet beam transport. Analytic solutions based on multi-time scale perturbation theory were found and compared to numerical simulations.

REFERENCES

- [1] *Special Issue on High-Power Microwave Generation*, edited by J.H. Booske, T.A. Spencer, and J.P. Verboncoeur, IEEE Trans. Plasma Sci., **28** (2000).
- [2] D.J. Radack, J.H. Booske, Y. Carmel, and W.W. Destler, Appl. Phys. Lett., **55**, 2069 (1989).
- [3] D. Yu and P. B. Wilson, in *Proceedings of 1993 Particle Accelerator Conference*, p. 2681 (1993).
- [4] J.H. Booske, A.H. Kumbasar, and M.A. Basten, Phys. Rev. Lett., **24**, 3979 (1993).
- [5] C. C. Cutler, J. Appl. Phys. **27**, 1028 (1956).
- [6] R. Pakter and C. Chen, Phys. Rev. **E62**, 2789 (2000).
- [7] Perhaps the most appropriate would be denoting as *short* and *long* longitudinal variations, instead of *slow* and *fast* variations, however since s and time are closely related by $s = \beta_b ct$, we decided to use the more usual terms *slow* and *fast* time-scales.